J1.5 PROTOTYPES FOR THE WRF (WEATHER RESEARCH AND FORECASTING) MODEL

W. C. Skamarock, J. B. Klemp and J. Dudhia

National Center for Atmospheric Research,*
Boulder, Colorado

1. INTRODUCTION

The Weather Research and Forecasting Model (WRF) is being developed in a collaborative effort by the National Center for Atmospheric Research (NCAR), the National Centers for Environmental Prediction (NCEP), the Forecast Systems Laboratory (FSL), the Air Force Weather Agency (AFWA), Oklahoma University (OU) and other university scientists. Our goal is to develop a state-of-the-art numerical weather prediction (NWP) and data assimilation system suitable for horizontal grid scales in the 1 to 10 km range. This modeling system will be used in both research and operational applications, and we believe that its development will lead to closer ties between the operational and research NWP groups and facilitate the transfer of new ideas and personnel between the research and operational communities.

There are three prototype dynamical cores under development in the WRF project; two Eulerian solvers that are described in this paper, and a semi-Lagrangian solver (Purser et al, 2001) described in another paper that can be found in this conference proceedings. The two Eulerian prototypes differ in their vertical coordinates, one uses geometric height as a vertical coordinate and the other uses mass (hydrostatic pressure). The height-coordinate prototype constituted the first public release of WRF Version 1.0 in November 2000. The release presents not only a prototype solver, but a model framework that specifically allows for parallel processing on distributed-memory, shared-memory, and hybrid (distributed-memory clusters of shared-memory nodes) computer architectures encompassing both scalar and vector computer architectures. This prototype is freely available to the community, and directions for downloading the model, along with descriptions and documentation about this WRF model release and the WRF model development effort can be found on the WRF Web site at *http://wrf-model.org.*

In this paper we briefly describe the Eulerian prototype cores, present both idealized and real-data simulation, and discuss plans for future development.

2. DYNAMICAL EQUATIONS

In developing the Eulerian prototypes, we have followed Ooyama's (1990) philosophy of formulating the prognostic equations in terms of variables that have conservation properties for both the height and mass coordinates. The resulting discrete models conserve mass, dry entropy and scalars to machine roundoff; exact momentum conservation is sacrificed for the efficiency of the split-explicit acoustic mode integration scheme. The primary difference in the Eulerian prototypes is the vertical coordinate, and the practical differences following from this are that the mass coordinate surfaces move whereas the height coordinate surfaces are fixed, and the upper boundaries conditions differ - the height coordinate model uses a rigid upper lid and the mass coordinate model uses constant pressure.

2.1 *Height Coordinate*

In the height coordinate model, the conservative form of the variables can be defined as

$$\mathbf{V} = \rho\mathbf{v} = (U, V, W), \quad \Theta = \rho\theta$$

and prognostic nonhydrostatic equations in conservative form without terrain are

$$\partial_t U + \nabla \cdot (\mathbf{v}U) + \gamma R\pi\partial_x\Theta' = F_U \tag{1}$$

$$\partial_t V + \nabla \cdot (\mathbf{v}V) + \gamma R\pi\partial_y\Theta' = F_V \tag{2}$$

$$\partial_t W + \nabla \cdot (\mathbf{v}W) + \gamma R\pi\partial_z\Theta' - g(\bar{\rho}\pi'/\bar{\pi} - \rho') = F_W \tag{3}$$

$$\partial_t\Theta + \nabla \cdot (\mathbf{v}\Theta) = F_\Theta \tag{4}$$

$$\partial_t\rho' + \nabla \cdot \mathbf{V} = 0. \tag{5}$$

Perturbation variables are defined as deviations from a time invariant hydrostatically balanced reference state such_that $p = \bar{p}(z) + p'$, $\rho = \bar{\rho}(z) + \rho'$, and $\Theta = \bar{\rho}(z)\theta(z) + \Theta'$. g is the acceleration due to gravity, $\gamma = c_p/c_v = 1.4$ is the ratio of the heat capacities for dry air. In arriving at this formulation, we have used the relation

$$\nabla p = \gamma R\pi\nabla\Theta,$$

and pressure is obtained from the diagnostic equation of state:

$$p = p_o \left(\frac{R\Theta}{p_o}\right)^\gamma. \tag{6}$$

In contrast to most existing compressible nonhydrostatic models, by integrating the equations (1)–(5), we do not integrate a prognostic pressure equation (typically an

* The National Center for Atmospheric Research is sponsored by the National Science Foundation.

Corresponding author address: Dr. William C. Skamarock, NCAR, P.O. Box 3000, Boulder, CO 80307-3000. email: *skamaroc@ucar.edu*

equation cast in terms of p or π). Instead, (4) takes the place of a pressure equation in the system. Since from (6) it is clear that pressure is just Θ raised to the power, γ, (4) can interpreted as a modified form of the pressure equation that has conservative properties. In the currently available WRF model, a terrain following coordinate is introduced along with the common map projections onto the sphere.

2.2 *Mass Coordinate*

Following the derivation by Laprise (1992), we represent the equations in terms of a terrain-following hydrostatic pressure vertical coordinate:

$$\eta = (p_h - p_{ht})/\mu \qquad \text{where} \quad \mu = p_{hs} - p_{ht} \tag{7}$$

where p_h is the hydrostatic component of the pressure, and p_{hs} and p_{ht} refer to values along the surface and top boundaries, respectively. Since $\mu(x, y)$ represents the mass per unit area within the column in the model domain at (x, y), the appropriate flux form variables become:

$$\mathbf{V} = \mu\mathbf{v} = (U, V, W), \quad \Omega = \mu\dot{\eta}, \quad \Theta = \mu\theta. \tag{8}$$

Using these variables, Laprise's (1992) equations can be written in terms of the prognostic equations:

$$\partial_t U + \left(\boldsymbol{\nabla} \cdot \mathbf{v}U\right)_\eta + \mu\alpha\partial_x p + \partial_\eta p \partial_x \phi = F_U \tag{9}$$

$$\partial_t V + \left(\boldsymbol{\nabla} \cdot \mathbf{v}V\right)_\eta + \mu\alpha\partial_y p + \partial_\eta p \partial_y \phi = F_V \tag{10}$$

$$\partial_t W + \left(\boldsymbol{\nabla} \cdot \mathbf{v}W\right)_\eta - g\left(\partial_\eta p - \mu\right) = F_W \tag{11}$$

$$\partial_t \Theta + \left(\boldsymbol{\nabla} \cdot \mathbf{v}\Theta\right)_\eta = F_\Theta \tag{12}$$

$$\partial_t \mu + \left(\boldsymbol{\nabla} \cdot \mathbf{V}\right)_\eta = 0 \tag{13}$$

$$\partial_t \phi + \left(\mathbf{v} \cdot \boldsymbol{\nabla}\phi\right)_\eta = gw \tag{14}$$

together with the diagnostic hydrostatic pressure equation

$$\partial_\eta \phi = -\mu\alpha \tag{15}$$

and gas law

$$p = \left(\frac{R\Theta}{p_0\mu\alpha}\right)^\gamma. \tag{16}$$

Again we cast the equations in terms of conserved variables, with the exception of the prognostic equation (14) which is a definition of the geopotential. Pressure is eliminated using the gas law as in the height coordinate system and we avoid integrating a non-conservative pressure equation, as in the height coordinate system.

2.3 *Solution Methods*

Both Eulerian prototypes use the split explicit solution procedure first described in Klemp and Wilhelson (1978) and in widespread use in many nonhydrostatic NWP models and research cloud models. We have introduced a third order accurate Runge-Kutta time integration scheme (Wicker and Skamarock, 2001) in place of the Leapfrog time discretization commonly used, and we use fifth order upwind discretizations for the flux divergence terms (advection) in the models. With these additions, we find that we can use timesteps typically twice as large as those used in the leapfrog models, and phase errors are noticeably reduced in comparison to the leapfrog formulations. We typically run these models without any explicit computational damping; there is some damping implicit in the Runge-Kutta scheme and the fith order upwind flux-divergence operators. Further information concerning the dynamical equations and the numerical methods used in the Eulerian models can be found at *http://www.mmm.ucar.edu/wrf/WG1.*

3. PHYSICS

WRF Version 1 includes a set of physics options sufficient to allow its use both in idealized and real-data simulations at a variety of grid sizes from cloud-resolving to mesoscale modeling applications. The current physics packages available in the Eulerian prototypes are:

- Microphysics
  - Kessler (no ice)
  - NCEP 3-class (simple ice)
  - NCEP 5-class (ice and snow)
  - Lin et al. (including graupel)
- Boundary Layer
  - MRF scheme (Hong and Pan)
- Surface Layer
  - Similarity theory
- Ground Layer
  - 5-layer soil thermal diffusion
- Subgrid 3D Turbulence/Diffusion
  - Constant diffusion
  - Smagorinsky type
  - TKE prediction (ARPS)
- Cumulus Parameterization
  - Kain-Fritsch
  - Betts-Miller-Janjic
- Radiation
  - RRTM longwave (Mlawer et al.)
  - MM5 shortwave (Dudhia)
  - Goddard shortwave (Chou)

There are plans for several more options in the near future including the Grell cumulus parameterization, the OSU land-surface model, the Reisner graupel microphysics, and the Eta model's Mellor-Yamada PBL scheme.

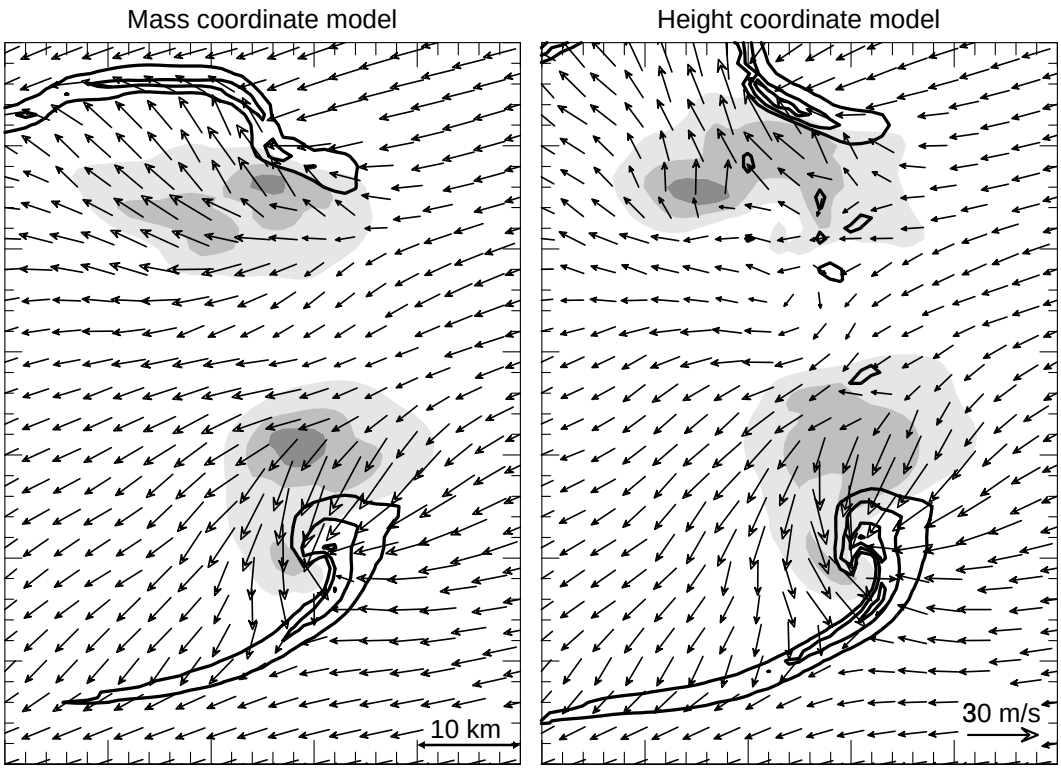

Figure 1. Splitting supercell simulation with the mass and height coordinate WRF prototypes.

4. REAL-DATA INITIALIZATION

The WRF Eulerian height-coordinate prototype possesses relaxation boundary condition for specified time-dependent analyses, map projections, and all Coriolis and curvature terms. Also, adequate physics are available in WRF for testing using real-data cases. A WRF software package called the the Standard Initialization (WRF SI), developed at the Forecast Systems Laboratory, is used to prepare an initial state and boundary conditions for WRF simulations of actual cases. The WRF SI takes standard Grib files of pressure-level data, defines a WRF grid, and interpolates the fields horizontally and vertically to the WRF grid. The WRF SI also provides terrain elevation, and vegetation class, and employs global datasets with 30" resolution (1 km) for these. This package is primarily an interpolating engine; it has no capabilities for ingesting site observations for an analysis. However, Grib is a widely used format, and the SI makes available several real-time and archived datasets of analyses both from regional and global models.

There is development work on a 3DVAR system for WRF. This is a collaborative effort amoung all the WRF partners to provide a means of improving the WRF initialization with a variety of observation types, including satellite measurements in addition to the standard synoptic platforms.

Currently this version of WRF is being run daily at NCAR (see the link on the WRF home page *http://wrf-model.org/*) and several other sites as a real-time forecast model. NCAR's real-time runs use a 30 km grid covering the United States with Eta initial and boundary conditions, and there are plans to regularly run a 10 km real-time run on a sub-area. The outputs from these efforts will be archived with the goal of evaluating the physics and dynamics of WRF by verifying the forecasts against observations.

5. IDEALIZED FLOW SIMULATIONS AND NWP TESTS

A number of initializations for idealized flow test cases are provided with the WRF model. The idealized flow test cases are well simulated by both the height- and mass-coordinate models and thus do not provide definitive evidence for discrimination between these prototypes. However, two of the test cases do demonstrate the multi-scale capabilities of the Eulerian WRF prototypes.

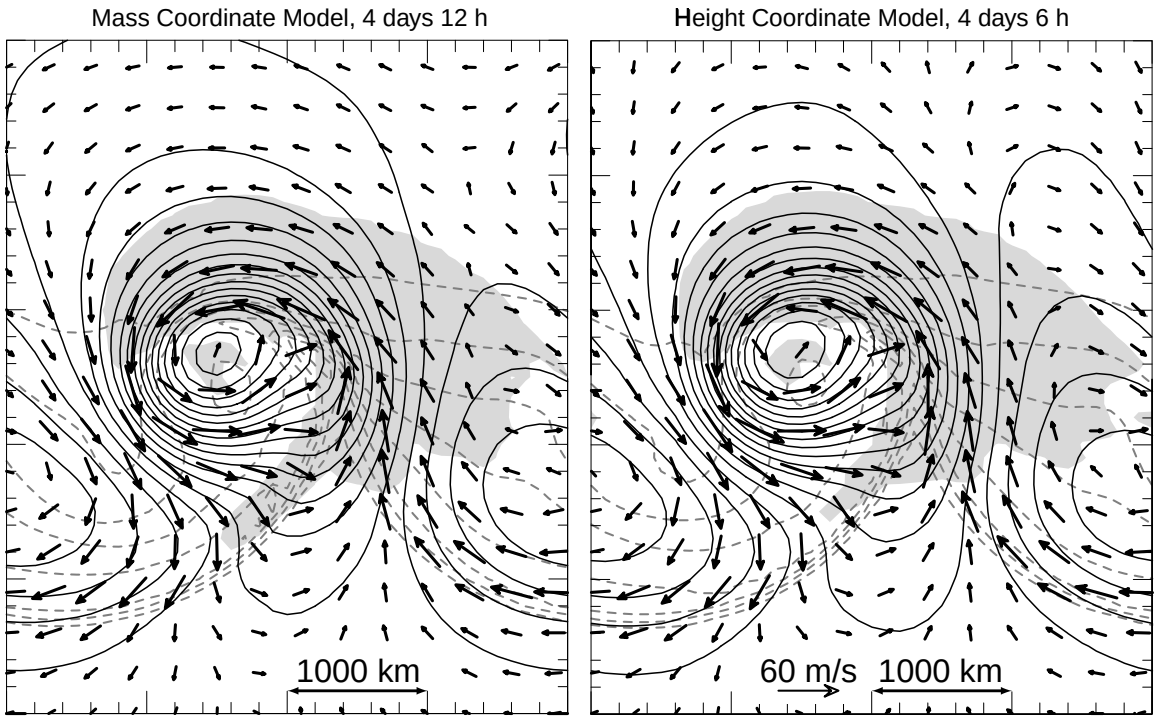

Figure 2. Baroclinic wave simulations with the WRF Eulerian prototypes.

The WRF model must be robust for cloud-scale simulations at high horizontal resolution; research NWP is closing in on the convection resolving scales, and operational NWP could be here by the end of this decade or sooner. As an example of the Eulerian prototypes' capability to robustly handle moist convection, we have simulated splitting supercell thunderstorm in a convectively unstable environment and a hodograph exhibiting clockwise curvature at low levels (see the quarter-circle shear supercell case described in Weisman and Rotunno 2000). The simulations used a timestep of 10 s on a grid with 1 km horizontal and approximately 500 m vertical resolutions in the two models. Maximum updrafts are greater than 50 m/s in the simulations, and a comparable leapfrog model would typically use a timestep of 6 s or less. Kessler microphysics are used in these simulations. Low-level circulations, updrafts, and rainwater fields are depicted for the right moving supercell and weaker left moving storm for both the mass and height coordinate models at 1.5 h in Figure 1. The hook-shaped rainwater field is wrapping around the occluding updraft at low levels and implies strong circulation, and is potentially a sign of tornadic activity. The subtle differences between the simulations are likely due to differences in the initializations (the vertical levels do not exactly coincide) and due to the different upper boundary conditions (rigid lid for the height coordinate prototype and constant pressure for the mass coordinate prototype).

The WRF model must also be robust at larger scales and coarser grid resolutions. As an example of the Eulerian prototypes' capability to robustly simulate synoptic-scale flows, we have performed simulations of moist baroclinic waves in a channel with the two Eulerian prototypes. The simulations of the baroclinically unstable jet are similar to that presented in Rotunno et al (1994). The simulations use a periodic channel of 4000x8000x16 km (E-W, N-S, z) and 100 km horizontal resolution and 250 m vertical resolution. The timestep used in the simulations is 600 s, again about twice as large as what would be used in a leapfrog-based model. Kessler microphysics and the Kain-Fritsch convective parameterization is used in these simulations, and the lower boundaries are free-slip. A snapshot of the developing synoptic wave is given in Figure 2. The models both reproduce the developing comma-shaped cloud fields along with the cold and warm frontal structure and the warm-core seclusion. Again, the differences between the simulations are likely due to the necessarily different initializations and upper boundary conditions.

As mentioned, the height coordinate WRF prototype is being evaluated using real-data NWP simulations. Because of our focus on model capability for resolutions

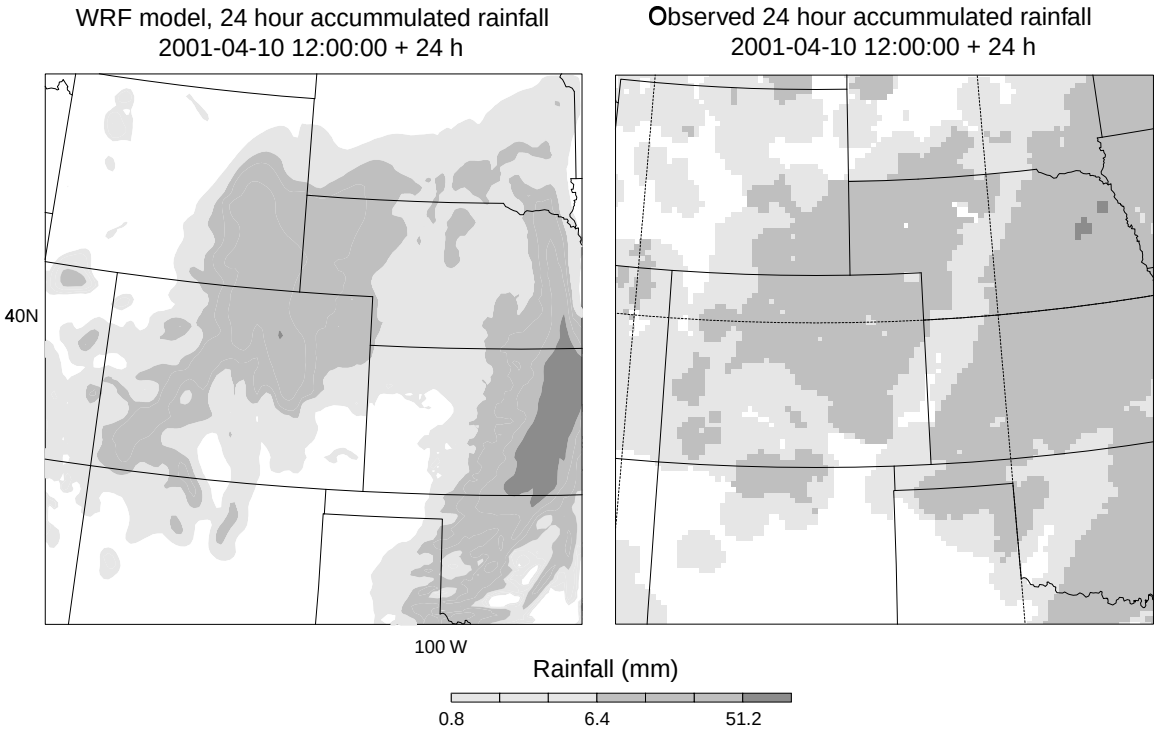

Figure 3. WRF height coordinate model precipitation accumulation forecast for the 24 hours preceding 12Z 11 April 2001. During this period a winter/spring storm has propagated out of the central Rockies onto the plains. The simulation was produced using a 10 km grid, and the verification observations are on a 15 km grid.

between 1 and 10 km, we are producing high resolution forecasts using a 10 km grid daily basis for portions of the central Rockies and central plains. We are also producing lower resolution forecast (30 km) over the continental U.S. for comparison with other mesoscale NWP forecast models. Figure 3 shows an example of a precipitation forecast for the 10 km horizontal forecast. The figure shows the 24 h accumulated precipitation along with verifying observations. The initial and boundary data for the forecast come from an 80 km ETA forecast, and the precipitation is accumulated over the first 24 h of the WRF forecast.

6. FUTURE PLANS

The development of the WRF prototypes will continue with addition of more advanced physics, development of the data assimilation system focusing on 3DVAR techniques, and flexible grid nesting procedures. It is our intent to continue testing the prototypes and, using idealized flow simulations and NWP tests, to narrow the development focus to a single prototype, while continuing development of promising prototypes in a research capacity for consideration as the future WRF dynamical core.

REFERENCES

Klemp, J. B., and R. Wilhelmson, 1978: The simulation of three-dimensional convective storm dynamics. *J. Atmos. Sci.*, **35**, 1070-1096.

Laprise, René, 1992: The Euler equations of motion with hydrostatic pressure as an independent variable. *Mon. Wea. Rev.*, **120**, 197-207.

Ooyama, K, V, 1990: A thermodynamic foundation for modeling the moist atmosphere. *J. Atmos. Sci.*, **47**, 2580-2593.

Purser, R. J., T. Fujita, S. K. Sar, and J. G. Michalakes, 2001: A semi-Lagrangian dynamical core for the non-hydrostatic WRF model. *Ninth Conference on Mesoscale Processes*, this conference proceedings.

Rotunno, R., W. C. Skamarock and C. Snyder, 1994: An analysis of frontogenesis in numerical simulations of baroclinic waves. *J. Atmos. Sci.*, **51**, 3373-3398.

Weisman, M. L., and R. Rutonno, 2000: The use of vertical wind shear versus helicity in interpreting supercell dynamics. *J. Atmos. Sci.*, **57**, 1452-1472.

Wicker, L. J., and W. C. Skamarock, 2001: Time Splitting Methods for Elastic Models Using Forward Time Schemes. *Mon. Wea. Rev.*, submitted, see *http://www.mmm.ucar.edu/individual/skamarock*.